Second Hydration Shell Single Scattering versus First Hydration Shell Multiple Scattering in $M(H_2O)_6^{3+}$ EXAFS Spectra

Hideto Sakane,[†] Adela Muñoz-Páez,*[,‡] Sofía Díaz-Moreno,[‡] José M. Martínez,[§] Rafael R. Pappalardo,[§] and Enrique Sánchez Marcos[§]

Contribution from the Department of Applied Chemistry and Biotechnology, Faculty of Engineering, Yamanashi University, 4-3-11 Takeda Kofu, Yamanashi 400-8511, Japan, Instituto de Ciencia de Materiales, Departamento de Química Inorgánica CSIC, Universidad de Sevilla, c/ Americo Vespucio s/n, 41092 Sevilla, Spain, and Departamento de Química Física, Universidad de Sevilla, 41012 Sevilla, Spain

Received December 5, 1997

Abstract: The analysis of the extended X-ray absorption fine structure (EXAFS) spectra of dilute aqueous solutions (0.1 M) of $Cr(NO_3)_3$ and $Rh(NO_3)_3$ was performed using several approaches. Single- and multiple-scattering (SS and MS) phenomena were taken into account to establish the relative importance of their possible contributions to the long distance peak ($R \approx 4$ Å). XANADU, FEFF, and FEFFIT codes were employed to analyze the data. The first approach considered the single-scattering contribution due to the existence of a well-defined second hydration shell around both of the trivalent cations, Cr^{3+} and Rh^{3+}. The second approach evaluated the contribution due to the multiple-scattering phenomena inside the first hydration shell. Comparison of experimental spectra with the calculated ones considering either one or both of the contributions led us to conclude that both contributions were significant in the high-R region of the spectra. This study supports our previous hypothesis which states that the second hydration shell structure can be obtained by EXAFS in these cations, although a quantitative analysis demands the inclusion of multiple-scattering phenomena inside the first hydration shell.

Introduction

The extended X-ray absorption fine structure (EXAFS) technique has been used during the last 20 years as a powerful tool for describing the near environment of atoms in condensed phases. In contrast to X-ray diffraction methods, this absorption technique needs neither long-range order in the system under study nor high concentrations of the species investigated. These advantages have led to its widespread use in the characterization of amorphous solids, highly dispersed catalysts, and biochemical structures containing metallic cations.[1,2] Likewise, ionic solutions seem appropriate environments for structural examination by EXAFS. However, the literature in this and other fields, such as electrochemistry, is scarce.[3,4] This is in part because of the generally accepted difficulty of obtaining structural information beyond the first coordination shell of the absorbing atom due to the sensitivity of EXAFS to disorder, which is usually higher in the liquid state than in the solid state.[5] Simple, well-defined aqueous solutions of highly charged metal cations such as Cr^{3+}, Rh^{3+}, Ga^{3+}, or Zn^{2+} seem particularly suited for investigations into whether this technique can supply structural information beyond the first hydration shell. Thus, we recently have shown experimental evidence by EXAFS of the presence of a second hydration shell for a set of transition metal cations in aqueous solutions over a wide range of concentrations.[6] Given that an EXAFS signal usually has an amplitude that represents 5−10% of the whole absorption edge jump and that the contribution due to the second hydration shell is not expected to be higher than 5−15% of the EXAFS amplitude, the ascription of this second shell contribution is a delicate and controversial subject.[7] In fact, the simultaneous concurrence of good quality data and the appropriate data analysis procedure is needed to determine this second shell. However, this capability is of general interest because it opens the door to obtaining additional structural information on the near environment of metal ions in solutions or in other electrochemical or biochemical media.

To deal with the structure around highly charged metal cations in aqueous solutions, some authors have argued that the small peak appearing in the Fourier transform (FT) of the EXAFS spectra at high R (ca. 4 Å) is due to the multiple-scattering (MS) phenomenon taking place within the first hydration shell.[8−10] However, the results of an analysis based on the assumption

* E-mail: adela@cica.es. Fax: 34-95-4460665.
[†] Yamanashi University.
[‡] Instituto de Ciencia de Materiales.
[§] Departamento de Química Física.

(1) Koningsberger, D. C., Prins, R., Eds. *X-ray Absorption: Principles, Applications, Techniques of EXAFS, SEXAFS and XANES*; Wiley: New York, 1988.
(2) Garner, C. D. *Adv. Inorg. Chem.* **1991**, *36*, 303.
(3) Sharpe, L. R.; Heineman, W. R.; Elder, R. C. *Chem. Rev.* **1990**, *90*, 705.
(4) Ohtaki, H.; Radnai, T. *Chem. Rev.* **1993**, *93*, 1157.
(5) Magini, M.; Licheri, G.; Paschina, G.; Piccaluga, G. *X-ray Diffraction of Ions in Aqueous Solutions: Hydration and Complex Formation*; CRC Press: Boca Raton, 1988.
(6) (a) Muñoz-Páez, A.; Sánchez Marcos, E. *J. Am. Chem. Soc.* **1992**, *114*, 6931. (b) Muñoz-Páez, A.; Pappalardo, R. R.; Sánchez Marcos, E. *J. Am. Chem. Soc.* **1995**, *117*, 11710. (c) Muñoz-Páez, A.; Díaz, S.; Pérez, P. J.; Martin-Zamora, M. E.; Martínez, J. M.; Pappalardo, R. R.; Sánchez Marcos, E. *Physica B* **1995**, *208 & 209*, 395.
(7) Read, M. C.; Sandstrom, M. *Acta Chem. Scand.* **1992**, *46*, 1177.
(8) Benfatto, M.; Natoli, C. R.; Bianconi, A.; Garcia, J.; Marcelli, A.; Fanfoni, M.; Davoli, I. *Phys. Rev. B* **1986**, *34*, 5774.
(9) Briois, V.; Lagarde, P.; Brouder, C.; Sainctavit, Ph.; Verdaguer, M. *Physica B* **1995**, *208 & 209*, 51.
(10) Filiponi, A.; D'Angelo, P.; Viorel Pavel, N.; Di Cicco, A. *Chem. Phys. Lett.* **1994**, *225*, 150.

S0002-7863(97)04142-5 CCC: $15.00
Published on Web 09/19/1998

that this peak is mainly due to the second hydration shell single scattering (SS)[6,11] agree reasonably well with structural information derived from other independent spectroscopic or diffraction techniques.[4,5,7,12] A peculiar characteristic which introduces ambiguity in this problem is the fact that the solvation structure around cations is such that the distance between the ion and the oxygen atoms of the second hydration shell is about twice the value corresponding to that of the first shell.[4] Thus, one or both of these contributions might be responsible for the long distance peak in the FT of the EXAFS spectra.

The development of refined algorithms that calculate single- and multiple-scattering contributions, such as the FEFF program,[13] coupled to appropriate fitting programs, such as FEFFIT,[14] and reasonable criteria to assign Debye−Waller (DW) factors to the different contributions compelled us to carefully revise the analysis of EXAFS spectra of the Cr^{3+} and Rh^{3+} aqueous solutions. These ions form two of the most stable hexahydrates in water and show two of the best defined second hydration shells.[4,5,12]

The aim of this work was to examine whether one, both, or neither of the above-mentioned contributions was responsible for the long distance peak of the FT of the EXAFS spectra for these two ionic aqueous solutions.

Experimental Measurements and Data Analysis

The Rh−K edge (22 228 eV) X-ray absorption spectrum of a 0.1 M aqueous solution of $Rh(NO_3)_3$ was measured at the 9.2 wiggler beamline at the SRS (Daresbury, U.K.). The ring energy was 2 GeV, and the ring current was 250 mA. A double-crystal Si(220), detuned 80% to reject higher harmonics, was used. The Cr−K edge (5989 eV) XAS spectrum of a 0.1 M aqueous solution of $Cr(NO_3)_3$ was measured at beamline BL-12C at the Photon Factory of the Institute of Materials Structure Science (Tsukuba, Japan), with a ring energy of 2.5 GeV and a ring current of 300 mA. A double-crystal Si(111) monochromator was used, followed by a Rh-coated Si focusing mirror. Higher harmonic rejection was carried out with a SiO_2 total reflection mirror. Energies were calibrated using Rh and Cr foils, for Rh−K and Cr−K edges, respectively. Energy resolution was estimated to be about 3 eV at the rhodium edge and 1.5 eV at the chromium edge. Measurements were carried out in transmission mode using optimized ion chambers filled with the appropriate gas mixtures (He/Ar and He/Kr for I_o and I_t when measuring the Rh−K edge; He/N_2 and N_2 for I_o and I_t when measuring the Cr−K edge) as detectors. Each datum point was collected for 1s, and several scans were averaged to minimize high- and low-frequency noise. In both cases, the aqueous solutions, at pH 1 to prevent hydrolysis, were placed in special liquid cells that enable the recording of highly corrosive media with different path lengths.[15]

Background subtraction was carried out by a procedure described elsewhere,[16] using the XANADU analysis package. Superimposed EXAFS signals were obtained by using the XDAP[17] program to perform background subtraction. The raw EXAFS data were analyzed with the FEFFIT software package,[14] using functions calculated with the FEFF 7.02 program[13] for the single- and multiple-scattering paths. Some FEFF and FEFFIT files used for Rh calculations are included as Supporting Information to allow for the reproduction of the results.

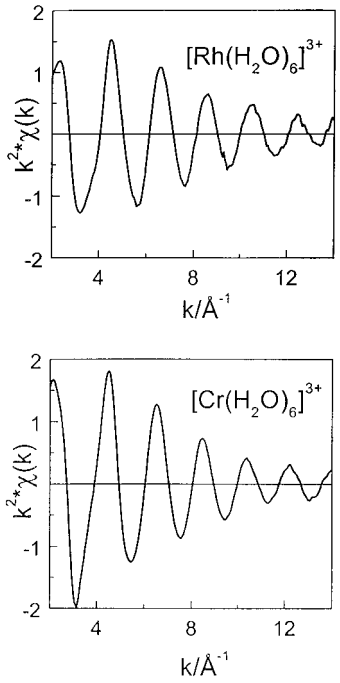

Figure 1. k^2-Weighted EXAFS spectra at the Rh− and Cr−K edges of 0.1 M $M(NO_3)_3$ (M = Rh, Cr) aqueous solutions.

The EXAFS spectrum of the solid crystalline hydrate $[Cr(NO_3)_3]\cdot 9H_2O$ of known structure[18] was used to determine the first shell Cr−O bond distance and the amplitude reduction factor S_0^2 and to test Debye−Waller (DW) factors.

Results and Discussion

Unfiltered and k^2-weighted EXAFS spectra of the Rh^{3+} and Cr^{3+} aqueous solutions have been plotted in Figure 1. It is worth noting that the data quality is excellent in both spectra and particularly good for the Cr^{3+} spectrum. The calculated uncertainties for Rh and Cr spectra are 1.6×10^{-4} and 3.5×10^{-5}, respectively, whereas spectra with noise levels on the order of 1.0×10^{-3} are usually considered "good" quality data. Both spectra show a rather simple wave, indicating that there is a dominant contribution, although the Rh^{3+} spectrum shows lower intensity at low k values.

The Fourier transforms, phase-shift-corrected for M−O contributions and plotted in Figure 2, show for Cr and Rh spectra a main peak centered at 2.0 Å and another smaller contribution centered at approximately 3.8 Å, with the latter stronger in the Cr^{3+} spectrum. The first peak corresponds to the SS contribution from the first hydration sphere. The coordination distances found for this contribution are 2.022 and 1.970 Å for the Rh−O and Cr−O signals, respectively, whereas the corresponding values for the DW factors are $\sigma^2_{\text{first SS}} = 0.0022$ and 0.0029 $Å^2$. Figure 2 also includes the results of the calculations described below.

To analyze the long distance peak, three different approaches were employed. Figure 3 includes all the paths considered in the three approaches: first and second shell SS paths and first shell MS paths. In the first approach, only the SS contribution from the second hydration sphere was considered, fixing the coordination number to the values previously determined by other techniques[4,12] (i.e., 12 for Rh and 14 for Cr) and leaving as free parameters the coordination distance and the DW factor for this shell. The second hydration shell can be roughly

(11) (a) Diaz-Moreno, S.; Muñoz-Páez, A.; Martinez, J. M.; Pappalardo, R. R.; Sánchez Marcos, E. *J. Am. Chem. Soc.* **1996**, *118*, 12654. (b) Martínez, J. M.; Pappalardo, R. R.; Sánchez Marcos, E.; Refson, K.; Díaz-Moreno, S.; Muñoz-Páez, A. *J. Phys. Chem. B* **1998**, *102*, 3272.

(12) Marcus, Y. *Ion Solvation*; Wiley: Chichester, U.K., 1986.

(13) Zabisnky, S. I.; Rehr, J. J.; Ankudinov, A.; Albers, R. C.; Eller, M. J. *Phys. Rev. B* **1995**, *52*, 2995.

(14) Stern, E. A.; Newville, M.; Ravel, B.; Yacoby, Y.; Haskel, D. *Physica B* **1995**, *208 & 209*, 117.

(15) Sánchez Marcos, E.; Gil, M.; Martínez, J. M.; Muñoz-Páez, A.; Sánchez Marcos, A. *Rev. Sci. Instrum.* **1994**, *65*, 2153.

(16) Sakane, H.; Miyanaga, T.; Watanabe, I.; Matsubayashi, N.; Ikeda, S.; Yokoyama, Y. *Jpn. J. Appl. Phys., Part 1* **1993**, *32*, 4641.

(17) Vaarkamp, M.; Linders, J. C.; Koningsberger, D. C. *Physica B* **1995**, *208* & *209*, 159.

(18) Lazar, D.; Ribar, B.; Divjanokovic, V.; Meszaros, Cs. *Acta Crystallogr.* **1991**, *47*, 1060.

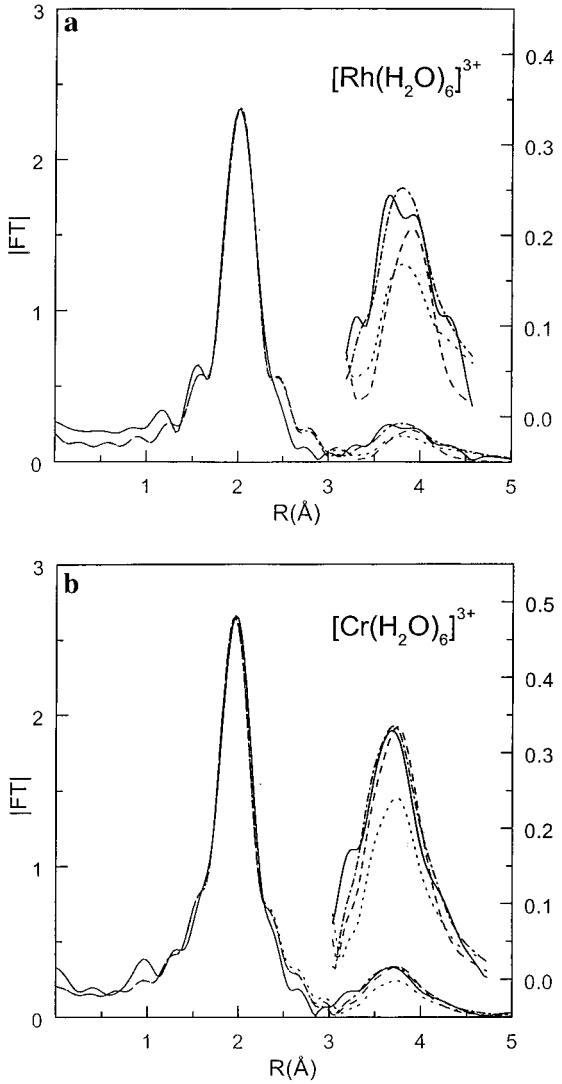

Figure 2. Magnitude of the phase-shift-corrected Fourier transform of the experimental and calculated EXAFS spectra of Rh^{3+} (a) and Cr^{3+} (b) aqueous solutions: experimental spectrum (solid line); best fits obtained with the parameters of Table 1 including single scattering (SS) contributions from the first and second hydration shells (dashed line); single- and multiple-scattering (MS) contributions from the first hydration shell (dotted line); SS and MS contributions from the first hydration shell plus SS contributions from the second hydration shell (dashed−dotted line). In all cases, the long distance peak magnitude has been multiplied by a factor of 6 (see right *y* axis).

described as formed by pairs of water molecules hydrogen-bonded to each water molecule from the first hydration shell. The HOH angle is ca. 105°, and the $M-O_I-O_{II}$ angle is expected to be around 130°, as shown in Figure 3. Thus even without taking into account the high values of the DW factors, MS effects from the second hydration shell are not expected to be relevant, because oxygen atoms in this shell are not aligned with those of the first shell. Moreover, the tilt angle[19,20] of the nearest water molecule would lead to further distortion of the structure. A fair reproduction of the second peak was obtained with this approach for the Cr^{3+} spectrum (dashed line in Figure 2b); however, that of Rh^{3+} (dashed line in Figure 2a) is worse. The DW factors obtained for the rhodium and chromium spectra were 0.0125 and 0.017 $Å^2$, respectively.

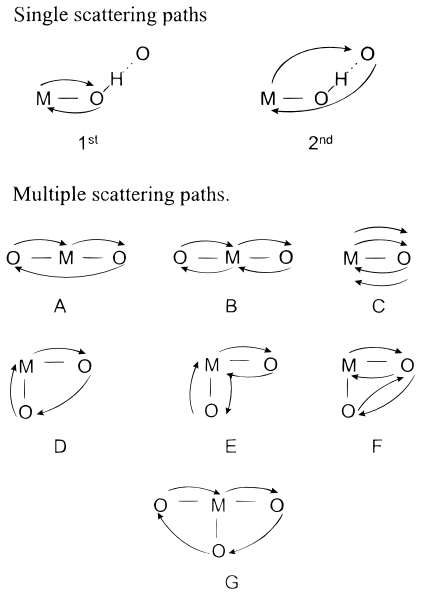

Figure 3. First and second hydration shell SS and MS paths within the first hydration shell of the hydrated cations.

In the second approach, only MS contributions from the first hydration shell were considered to reproduce the second peak. The results of the FEFF calculations with a plane-wave amplitude filter of 2.5% yielded the seven (A−G) MS paths included in Figure 3. The first three correspond to the three- and four-legged paths appearing in the linear arrangement O−M−O. The other four are the three- and four-legged paths involving cis oxygen atoms around the metal center.

To reduce the number of free parameters, an independent vibration approximation model[21,22] was considered. According to this model, the DW factors for these MS paths were not free parameters, but rather they were defined as functions of SS M−O and O−O DW factors. When this noncorrelated motion model was taken into account, only A, B, and C paths, including aligned atoms O−M−O, showed a DW factor small enough to yield a significant EXAFS contribution. In contrast, the triangular paths (D−G) have a very high DW factor, and their contribution to the EXAFS signal is thus negligible.[22,23] There were no variables in this approach.

According to this model, the DW factor for path C (twice single scattering) equals 4 times the value of the M−O SS path, $\sigma^2_C = 4\sigma^2_{\text{first SS}}$. There is not a similar simple relationship for DW factors for paths A and B, but their values are approximately twice those of the corresponding M−O SS paths, $\sigma^2_{A,B} \approx 2\sigma^2_{\text{first SS}}$.[21] The MS contributions calculated in this way for the Rh^{3+} and Cr^{3+} EXAFS spectra have been plotted in Figures 4a and 5a, respectively. As shown there, the most intense linear paths, A and B, are opposite in phase, so they partly cancel each other, and the amplitude of the sum of the three contributions (solid lines plotted in Figures 4b and 5b) is much smaller than expected. A similar effect has been observed in the mercury dihalides[21] as well as in the platinum hexahalides[23] and should appear in all systems of the type X−A−X showing a trans arrangement of the backscattering atoms (X) with the absorbing one (A), regardless of the DW factors used. As a consequence, the amplitude of the high-*R* peak obtained

(19) Martínez, J. M.; Pappalardo, R. R.; Sánchez Marcos, E. *J. Chem. Phys.* **1998**, *109*, 1445.
(20) Broadbent, R. D.; Nielson, G. W.; Sandstrom, M. *J. Phys.: Condens. Matter* **1992**, *4*, 639.
(21) Yokoyama, T.; Kobayashi, K.; Ohta, T.; Ugawa, A. *Phys. Rev. B* **1996**, *53*, 6111.
(22) Haskel, D. Ph.D. Thesis, University of Washington, Seattle, WA, 1998.
(23) Yokoyama, T.; Yonanoto, Y.; Ohta, T. *Phys. Rev. B* **1996**, *54*, 6921.

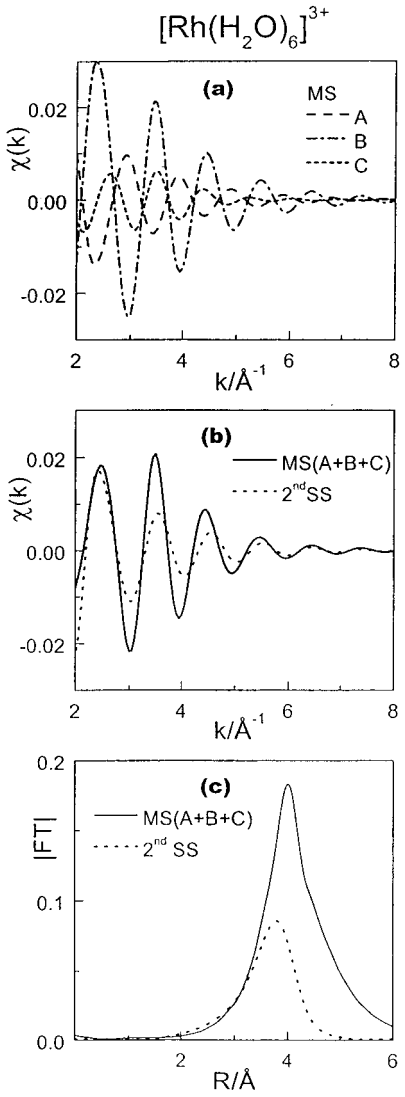

Figure 4. EXAFS contributions to the long distance peak, calculated with the parameters used in the third approach for the rhodium spectrum (see Figure 3 for path identification): (a) contributions from MS paths A (dashed line), B (dashed−dotted line), and C (short dashed line); (b) sum of MS paths A + B + C (solid line) and SS contribution from the second shell (dotted line); (c) phase-corrected Fourier transform of the curves included in part b of this figure.

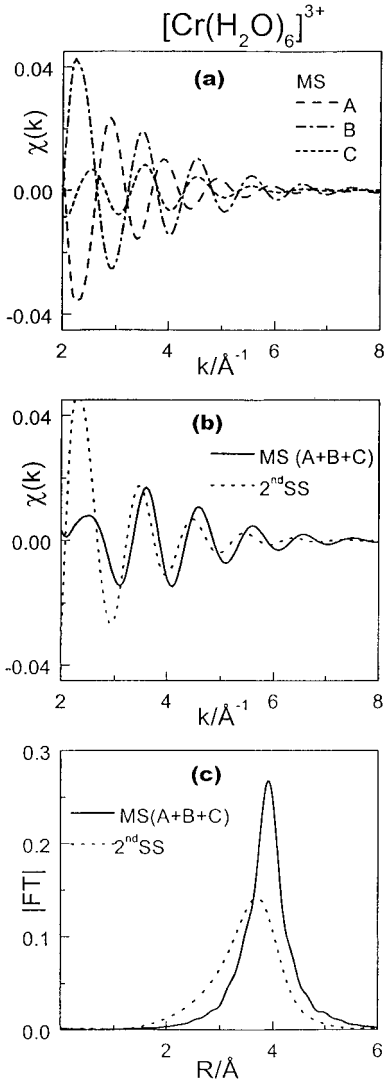

Figure 5. EXAFS contributions to the long distance peak, calculated with the parameters used in the third approach for the chromium spectrum: (a) contributions from MS paths A (dashed line), B (dashed−dotted line), and C (short dashed line); (b) sum of MS paths A + B + C (solid line) and SS contribution from the second shell (dotted line); (c) phase-corrected Fourier transform of the curves included in part b of this figure.

in such a way was smaller than the experimental one in both spectra, as plotted in Figure 2 (dotted line).

In the third approach, both types of contributions were included in the FEFFIT analysis with the restrictions mentioned above: fixed coordination numbers for the second shell and DW factors for MS contributions within the first coordination sphere defined as functions of SS contributions. Two variables per fit were used in this approach. As expected, the best reproduction of the EXAFS spectra was achieved with this approximation (see Figure 2), although the improvement was more significant in Rh^{3+} than in Cr^{3+} (cf. R factor and χ_ν^2 values in Table 1 and Cr^{3+} and Rh^{3+} spectra in Figure 2, dashed−dotted line). An additional difference between both systems was the increase in the coordination distance of the second hydration shell observed for Cr^{3+} when the two contributions were considered, while no changes were detected for Rh^{3+}. Parts b and c of Figures 4 and 5 include comparative plots of the second shell SS and the sum of first shell MS contributions in k and R spaces. Since the DW factors for MS contributions were fixed, their amplitudes were not modified by the inclusion of the second hydration shell contribution. On the contrary, the DW factors for the second shell SS contributions were multiplied by a factor

Table 1. Fitting Parameters for Rh^{3+} and Cr^{3+} EXAFS Spectra (k^2 Fit)

		approach used		
		second shell SS[a]	first shell MS[b]	second shell SS + first shell MS[a]
$Rh(H_2O)_6^{3+}$ [c]	R_{second} (Å)	3.99 ± 0.03		3.98 ± 0.05
	$\sigma^2_{second\ SS}$ (Å^2)	0.0125 ± 0.004		0.028 ± 0.011
	$\sigma^2_{first\ MS}$ (Å^2)		0.0045	0.0045
	R factor	0.015	0.015	0.013
	χ_ν^2	259	203	174
$Cr(H_2O)_6^{3+}$ [d]	R_{second} (Å)	3.87 ± 0.016		3.97 ± 0.036
	$\sigma^2_{second\ SS}$ (Å^2)	0.017 ± 0.003		0.032 ± 0.008
	$\sigma^2_{first\ MS}$ (Å^2)		0.0057	0.0057
	R factor	0.011	0.012	0.010
	χ_ν^2	2988	4154	2692

[a] Fitted variable = 2. [b] Fitted variable = 0. [c] $Rh(H_2O)_6^{3+}$: R_{Rh-O} = 2.022 Å; $\sigma^2_{first\ SS}$ = 0.0022 Å^2; S_0^2 = 1; Δk = 2.7−12.7 Å^{-1}; ΔR = 0.8−4.3 Å; ΔE_0 = −0.2 eV. [d] $Cr(H_2O)_6^{3+}$: R_{Cr-O} = 1.970 Å; $\sigma^2_{first\ SS}$ = 0.0029 Å^2; S_0^2 = 0.885 (determined from the spectrum of crystalline hydrate[18]); Δk = 2.8−13.7 Å^{-1}; ΔR = 0.9−4.1 Å; ΔE_0 = −2.1 eV.

of approximately 2 after the inclusion of first shell MS contributions (third approach).

The parameters used in the fits—metal−oxygen bond distance R_{second} (variable), DW factors for MS (fixed) and SS (variable) contributions, $\sigma^2_{first\ MS}$ and $\sigma^2_{second\ SS}$, and additional information such as the amplitude reduction factor, S_0^2, inner potential correction, ΔE_0, and fitting ranges for the three approaches—are shown in Table 1. In addition to the comparative plots, estimates of fit quality were given by R factors and χ_ν^2 values, calculated as defined in ref 14. In both metals, the smallest value of both parameters was obtained for the third approach, thus indicating that this is the best fit. The values of the R factor are very similar for the first and second approaches, but significant differences can be found in χ_ν^2 for both approaches. As shown in Table 1, this value is 20% smaller for the second approach in the case of rhodium and 25% smaller for the first approach in the case of chromium. Thus, if a single contribution had to be chosen to fit the long distance peak, it should be the MS contribution in the $[Rh(H_2O)_6]^{3+}$ spectrum and the second shell SS contribution in the $[Cr(H_2O)_6]^{3+}$ spectrum.

Interestingly, in either the first or the second approach, the fit improved slightly when the restrictions were not considered, i.e., in the MS approach when the DW factor was left free and in the second shell SS approach when the coordination number was left free. Results without physical meaning were obtained in both cases, that is, a very small DW factor for MS contributions and a very high coordination number for the second coordination sphere. According to this data analysis procedure, the second shell coordination number cannot be obtained due to the small sensitivity of the fitting function to this parameter and to the appearance at a similar distance of two independent contributions.

From all these results, we conclude that the high-R peak in the EXAFS spectra of the Rh^{3+} and Cr^{3+} aqueous solutions is due both to MS phenomena within the first coordination sphere and to SS phenomena from the second coordination shell, because these contributions are significant in this region of the spectrum. For these aquaions, the octahedral structure leads to the appearance of MS paths whose important contributions to the EXAFS signal are mutually canceled to a large extent. This helps to maintain the importance of the second hydration shell single-scattering contribution. Surprisingly, this contribution was different in the Cr^{3+} and Rh^{3+} spectra, although the structure and kinetic stability of both aquaions are very similar. This difference should be due to an atomic effect related to the change in the absorber and is probably related to the differences in phase-shift functions for Cr and Rh. This study supports our previous hypothesis[6] that the second hydration shell structure could be obtained by EXAFS in cations such as Cr^{3+} and Rh^{3+} which form a kinetically stable hexahydrate,[4,12] although some structural information derived from other techniques and the inclusion of multiple-scattering contributions inside the first hydration shell are required for a quantitative analysis.

Acknowledgment. This work has been performed under the approval of the Photon Factory Advisory Committee (Proposal 95G-215) and the SERC-SRS Advisory Committee (Proposal 23/338), with financial support of the Spanish DGICYT (PB95-0549) and the Yamada Science Foundation. Prof. J. Rehr is acknowledged for the use of his program, and he and Prof. I. Watanabe are acknowledged for helpful discussions. Dr. Newville is thanked for his helpful advice on the use of the FEFFIT program.

Supporting Information Available: FEFF input file (Table S1), FEFF output files PATHS.DAT (Table S2), FILES.DAT (Table S3), FEFFIT input file (Table S4), and fit parameters for the three approaches (Table S5) (5 pages, print/PDF). See any current masthead page for ordering information and Web access instructions.

JA974142D